

# Diffusion of Feed Spray in Fluid Catalytic Cracker Riser

Yiping Fan, Chenglin E, Mingxian Shi, Chunming Xu, Jinsen Gao, and Chunxi Lu  
State Key Laboratory of Heavy Oil Processing, China University of Petroleum, Beijing 102249, P.R. China

DOI 10.1002/aic.12035

Published online August 24, 2009 in Wiley InterScience (www.interscience.wiley.com).

*For fluid catalytic cracker (FCC) riser reactor, the diffusion pattern of feed spray and the flow features of catalysts in the feed injection zone were investigated in a cold-riser model that is made of 186-mm ID plexiglass pipe. In the feed injection zone, when a feed spray is introduced into the riser, a secondary flow of spray will occur. The secondary flow extends at first and then merges into the mainstream of spray. The occurrence of the secondary flow enhances the mixing of catalysts with feed. However, the extension of the secondary flow causes a violent catalyst backmixing; it is believed to be harmful to FCC reaction. The generation of the secondary flow of feed spray was theoretically analyzed by using the Kutta-Joukowski Lift Theorem. Furthermore, a FCC feed nozzle, which can controll/utilize the secondary flow in riser, was proposed. The effects of the nozzle used in some commercial FCC units are quite desirable.*

© 2009 American Institute of Chemical Engineers *AICHE J*, 56: 858–868, 2010

**Keywords:** multi-phase flow, diffusion, circulating fluidized beds, reactor analysis, petroleum

## Introduction

The fluid catalytic cracker (FCC) is the primary conversion unit in most refineries. It is reported that about 45% of worldwide gasoline productions come either directly from FCC units or indirectly from combination with downstream units.<sup>1</sup> In the feedstock injection zone of a FCC riser reactor, feed oil is introduced into the riser through the atomizing nozzles, and the feed comes in contact with the high-temperature catalysts and then reacts rapidly. In a commercial FCC unit, the goal is to ideally contact the catalysts with feed oil in the riser reactor under optimal operating conditions for a maximum yield in gasoline, LPG, and diesel. However, the hydrodynamics of gas–solid flow in the feed injection zone of FCC riser is very complex, which can be described by multiple confined jets injecting into a 3D, three-phase flow. Relevant research on the flow patterns of catalyst feed in this zone, especially the experimental research, is quite limited.

Chen<sup>1</sup> introduced the radial temperature profiles of a commercial FCC riser right above feed injection; it shows that the contact of feed with catalysts is rather nonuniform. Helmsing et al.<sup>2</sup> investigated the residence time distribution and Peclet number of catalysts in a microriser reactor. However, because their experimental reactor is too small (4-mm ID), the detailed hydrodynamics in the feed injection zone cannot be obtained. In the same experimental setup, Dupain et al.<sup>3</sup> proposed a lumped kinetic scheme to describe the observed phenomena; calculations on the feed reactivity and mass transfer have been made. Mcmilan et al.<sup>4</sup> have used both temperature and triboelectric measurements to determine the liquid/solid distribution in the feed injection area, however, their experiments were conducted in a dower chamber, not the commonly used riser. Fan et al.<sup>5</sup> have employed hydrogen tracer and optical fiber probe to study the flow patterns of catalysts and nozzle spray in the feed injection zone of the riser. However, their experimental results, in particular, the generation of the secondary flow of the feed spray in the feed injection zone should be further theoretically explained.

Numerical simulation is one of the most significant means by which a comprehensive understanding of the gas–solid

Correspondence concerning this article should be addressed to C. Lu at lcx725@yahoo.cn

flow in the feedstock injection zone can be achieved. The logs et al.,<sup>6–9</sup> Gao<sup>10</sup> have incorporated the lumped kinetic models into 3D computational fluid dynamics techniques. Even the simulation of feed vaporization (or atomization) inside the riser was addressed in detail. In addition, Albrecht et al.<sup>11</sup> performed an unsteady simulation of three-phase gas-droplet-particles turbulent flow with heat and mass transfer in the feedstock injection zone of an commercial FCC riser using a two-fluid modeling approach. The relevant configurations for further investigation with LES simulation, combined with deterministic Lagrangian tracking, are defined.

The numerical simulation, however, is too complex for engineering purposes. Moreover, some boundary conditions and initial conditions in the simulation cannot be precisely given. They have to be determined by experiment.

To enhance the contact of catalysts with feed droplets, some patents covering the riser internals,<sup>12–14</sup> as well as the new generation of FCC nozzle,<sup>15–18</sup> whose feed injection angle is adjustable have been put forward. However, these techniques are essentially tentative works. In other words, they are not based on the detailed study on the hydrodynamics of gas–solid flow in the feed injection zone.

In this article, the flow features of catalysts and the diffusion pattern of feed spray in three different-structure feed injection zones were experimentally investigated. The most noticeable phenomenon of the spray diffusion, i.e., the generation of the secondary flow of feed spray was theoretically analyzed. In addition, a new FCC feed nozzle that can control/use the secondary flow in riser was introduced.

## Experimental Setup and Measurements

### Experimental setup

The experimental setup is shown in Figure 1. It is mainly composed of a riser system, a gas–solid separation system, and a recirculation system. The riser is a plexiglass pipe with an ID of 186 mm and height 12 m. The feed injection zone is installed at a height of 4.5 m above the prelift gas distributor. Four nozzles are equipped with an angle of 30° relative to the riser axis, the same as in most industrial units. The gas–solid separation system includes two stages of cyclones. The recirculating system consists of a plexiglass downer of 500-mm ID equipped with a butterfly valve for measuring the solid flux. The solid flux is calculated by measuring the time for a known volume of particles to accumulate on the butterfly valve after the valve is closed.

The prelift gas, the feed spray, and the fluidizing gas are atmospheric air and are all supplied by the Roots' blowers. Their flowrates are controlled by a series of rotameters. The superficial velocities of the prelift gas and of the nozzle spray range from 3.28 m/s to 4.30 m/s and 41.7 m/s to 83.3 m/s, respectively; while the solid flux in the riser is controlled in a range from 70 to 390 kg/m<sup>2</sup>s. The particles are typical FCC catalysts. The particle density  $\rho_p$  is 1310 kg/m<sup>3</sup>, while the mean diameter  $d_p$  is 65  $\mu$ m.

Three investigated feed injection zones are shown in Figure 2. The No. 1 is a traditional structure, which can be characterized by an equivalent diameter pipe, as illustrated in Figure 2A. The No. 2 is shown in Figure 2B. In this feed injection scheme, an inner Louver conduit is set exactly

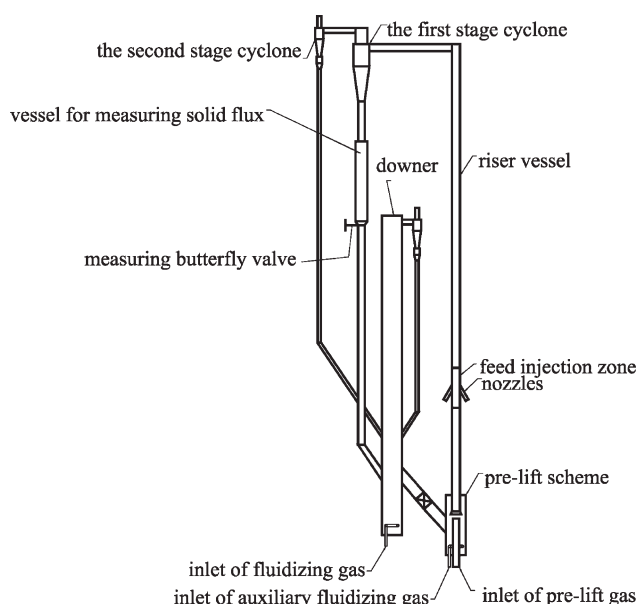


Figure 1. Experimental setup.

above the nozzles. The attack angle of the Louver conduit  $\alpha$  is 2.5° relative to the riser axis, which is equivalent to the flow angle of the secondary flow of feed spray in riser.<sup>5</sup> The divergence angle of the Louver conduit  $\beta$  is 7°, which is the same as a free jet. In the No. 3 feed injection zone, four inner baffles are fixed exactly above four nozzles. The attack angle and the divergence angle of the baffle, i.e.,  $\alpha$  and  $\beta$  in Figure 2C, are 2.5° and 7°, respectively. In the No. 2 and No. 3 feed injection zones, the lengths of the Louver conduit and of the baffles are  $L = 0.5$  m.

### Measurements and data analysis

A hydrogen-tracer technique is used to study the diffusion and flow characteristics of feed spray after it is injected into the riser. The cross-sectional distributions of the hydrogen concentration and of the hydrogen residence time are investigated at five axial heights of riser. The local density and the local axial particle velocity at different positions inside the riser are measured with the optical fiber probes.

*Eigen-Concentration and Eigen-Velocity of Feed Spray.* The concentration of the tracer at  $i$  location,  $C_i$ , can be obtained directly by the sampling system. However, the sampled  $C_i$  cannot be directly used to characterize the cross-sectional distributions of feed spray. It is because of the following:

1. In this research, the hydrogen tracer injection into the nozzles is pulse (not continuous injection); in other words, the injection time is very transient (30 ms), and the flowrate of the tracer is much less than those of the prelift gas and nozzle spray gas at each location. Because of the intense turbulence of gas–solid flow in a riser, the measured concentrations of the tracer vary inevitably even if at a fixed operating condition.

2. The tracer concentration,  $C_i$ , was measured with an online chromatogram. It can only quantify the concentration of the hydrogen in the sampled pure gas, rather than that in two-phase flow. That means the volume of the particles is not considered if using a chromatogram.

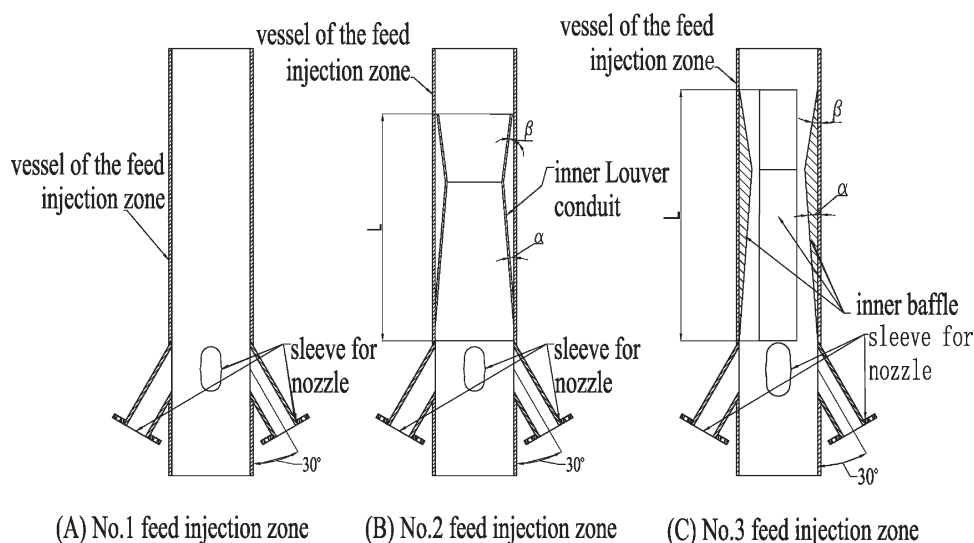


Figure 2. Three different feed injection zones.

3. The most idealized tracer injection is using pure hydrogen as the nozzle spray. However, it is really an impossible task for safe and economical reasons.

Therefore, a parameter  $\bar{C} = \frac{C_i/(1 + \varepsilon_{pi})}{\Sigma[C_i/(1 + \varepsilon_{pi})]} (Q_j/Q_j + Q_R)$  is introduced in this article. It is named by Eigen-concentration of tracer. Here  $\varepsilon_{pi}$  means the local volume fraction of the solid phase measured at the location where the tracer concentration is also investigated. Introduction of  $(1 + \varepsilon_{pi})$  is to characterize the actual concentration of the tracer in two-phase mixture. For describing conveniently, we call  $C_i/(1 + \varepsilon_{pi})$  as the two-phase concentration of the tracer. In this research,  $\varepsilon_{pi}$  is obtained with the optical fiber probe.  $\Sigma[C_i/(1 + \varepsilon_{pi})]$  denotes the sum of all the two-phase concentrations of the tracer, which are measured at different cross-sectional locations at an investigated axial height. The term  $\frac{Q_j}{Q_j + Q_R}$  is to modify the difference between the idealized continuous injection of pure hydrogen and the pulse injection. It is like that a  $Q_j$  volume of solute is dissolved in a  $Q_j + Q_R$  volume of solution.

The parameter  $\bar{C}$  reflects the relative concentration of feed spray at different locations in the riser after it is injected into the riser.

The Eigen-velocity of spray, which is defined by  $u_e = k/t$ , reflects the relative velocity of feed at different positions in the riser. The parameter  $t$  denotes the mean residence time of the hydrogen tracer at the sampling position, which can be directly obtained through the sampling system, while the number  $k$  is a constant.

**Measurement of Local Density.** The local density is measured with a PC-4 optical fiber probe that is supplied by the Institute of Processing Engineering, Chinese Academy of Sciences, Beijing, China. When a beam of light irradiates on a cluster of particles, part of the light will be reflected, whereas the other part will be absorbed. The principle of an optical fiber probe is based on the fact that the intensity of reflected light depends on the concentration of the particles irradiated.

The probe is 3.8 mm in diameter and contains thousands of emitting and receiving quartz fibers, each of diameter 15  $\mu\text{m}$ . More details of the probe have been presented elsewhere.<sup>5</sup> Similar probe was also introduced by other researchers.<sup>19</sup>

**Measurement of Particle Velocity.** The particle velocity is measured by using a PV-3 optical fiber probe that is also supplied by the Institute of Processing Engineering, Chinese Academy of Sciences, Beijing, China. In this instrument, five parallel fibers of diameter 200  $\mu\text{m}$  are placed in a stainless-steel tube. A particle moving through any two neighboring fibers will produce reflective signals that can be detected by the fibers. By counting the shift times of these signals, the local particle velocity is determined. The stainless-steel tube consists of a horizontal cylindrical portion of 2-mm OD and length about 0.3 m, leading to a 10-mm-long tip of oval-shaped cross-section of 0.5 mm wide by 1.8 mm high. This optical fiber probe was used elsewhere before.<sup>5</sup> Similar probe was also described by others.<sup>20</sup>

The local particle velocities measured with the optical fiber probe indicated that particles inside a riser move upward and downward dynamically wherever the radial location is. Even in the upper part of the riser, the downflow of the particle can be detected in the central region. Because the proportion and magnitude of the upflowing particles are different from those of the downflowing particles, the arithmetical average of the particle velocities is different at different locations. In fact, the granular flow in a riser is not a continuous flow from a strict Euler viewpoint. The arithmetical average velocity of particles at a given position is

expressed by  $V_p = \frac{n_u V_u - n_d V_d}{n_u + n_d} = \frac{\sum_{i=1}^N \vec{V}_{pi}}{N}$ , where  $n_d$  is the number of the particles whose velocities are downward;  $n_u$  is the number of the particles whose velocities are upward;  $V_d$  is the arithmetical average velocity of particles whose velocities are downward;  $V_u$  is the arithmetical average velocity of particles whose velocities are upward;  $\vec{V}_{pi}$  is the velocity vector of any particle  $i$ . The parameters  $n_d$ ,  $V_d$ ,  $n_u$ , and  $V_u$  can be directly measured with the optical fiber probe.

As an intrusive technique, the optical fiber probe may bring about errors in particle velocity and local density measurements, because the probe interferes with the flow inevitably. Unfortunately, nobody has ever estimated the errors caused by the intrusion of probe. However, Werther et al.<sup>21</sup> have directly compared the results of optical fiber

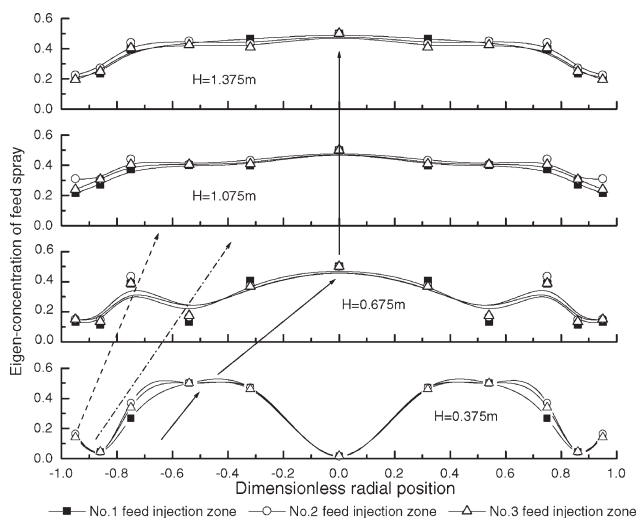


**Figure 3. Radial distributions of the Eigen-concentration of feed spray in three different feed injection zones.**

probe and LDA under identical operating conditions in a circulating-fluidized bed riser. The good agreement of the local solid velocities acquired with the two systems indicated that the probe causes negligible distortion of the solid velocity patterns in a riser. At present, the optical fiber probe is an effective technique in measuring local density and particle velocity, especially for dense phase.

**Particle Backmixing Ratio.** This parameter is defined by the value of  $\gamma = \frac{n_d \times V_d}{n_u \times V_u}$  at the investigated location. The particle backmixing ratio reflects the momentum ratio of the particles whose velocities are downward to those of the upward particles. A higher particle backmixing ratio denotes a more intense collision among particles, which inevitably results in a longer residence time. It is believed that the long residence time of catalysts in feed injection zone closely relates to some undesirable byproduct such as coke and dry gas.

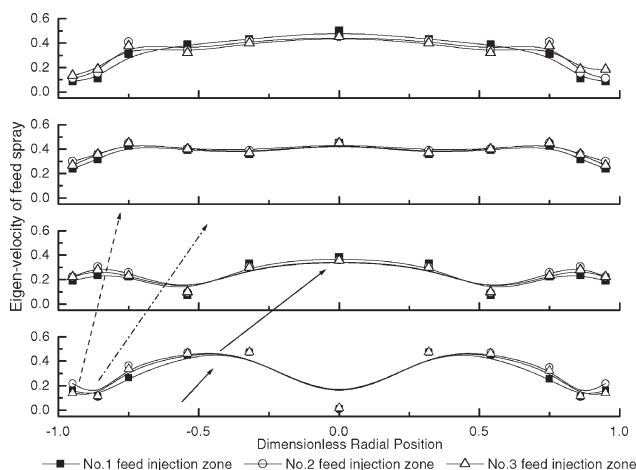


**Figure 4. Radial distributions of Eigen-velocity of feed spray in three different feed injection zones.**

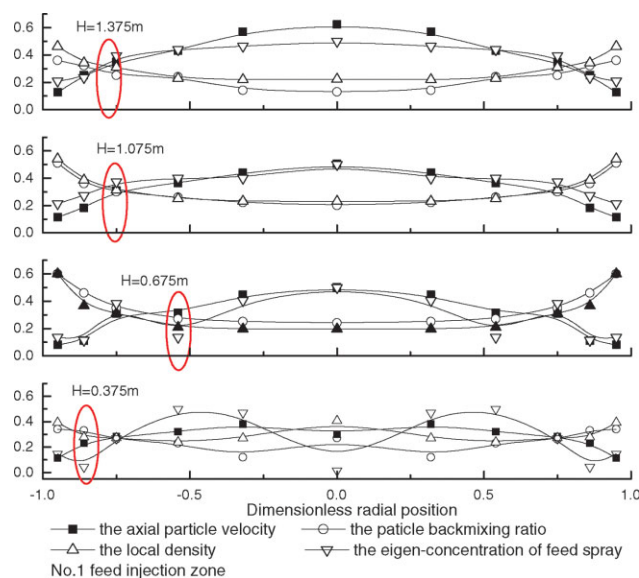


**Figure 5. All the investigated parameters at different axial heights in the No. 1 feed injection zone.**

[Color figure can be viewed in the online issue, which is available at [www.interscience.wiley.com](http://www.interscience.wiley.com).]

## Experimental Results

### The diffusion of feed spray in the feed injection zone

Figures 3 and 4 show the radial profiles of the Eigen-concentration  $\bar{C}$  and the Eigen-velocity  $u_e$  of feed spray. In these two Figures (as well as in Figures 5–7 in the following text), a representative operating condition is taken in which the nozzle spray velocity is 62.5 m/s, the superficial prelift gas velocity is 4.3 m/s, while the solid flux in the riser is 390 kg/m<sup>2</sup>s.

In these three different feed injection zones, the hydrogen tracer was not detected at the height below the nozzles

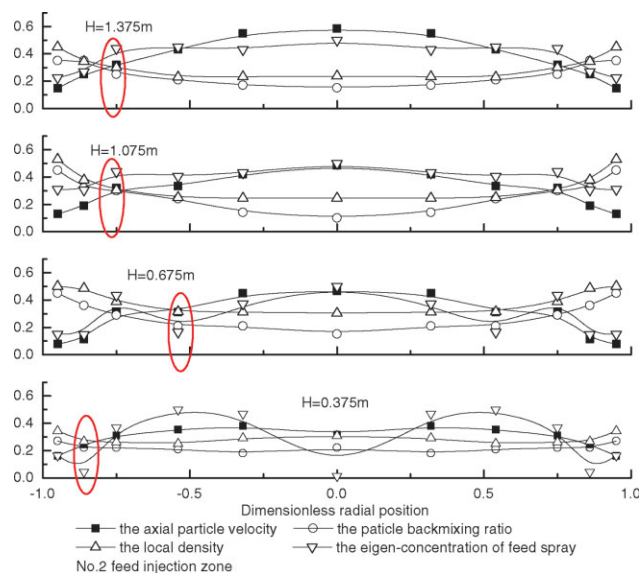


**Figure 6. All the investigated parameters at different axial heights in the No. 2 feed injection zone.**

[Color figure can be viewed in the online issue, which is available at [www.interscience.wiley.com](http://www.interscience.wiley.com).]



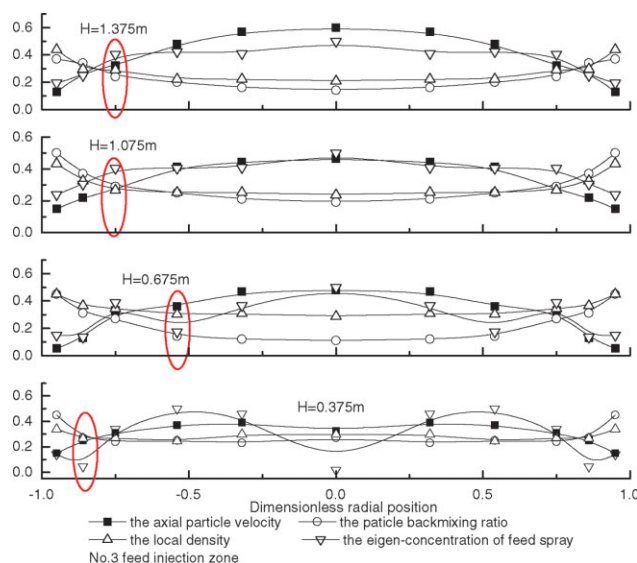


**Figure 7. All the investigated parameters at different axial heights in the No. 3 feed injection zone.**

[Color figure can be viewed in the online issue, which is available at [www.interscience.wiley.com](http://www.interscience.wiley.com).]

0.2 m. This demonstrates that in a riser, there is no large-scale backmixing of feed spray upstream the nozzles.

At  $H = 0.375$  m above the nozzles, the minimum of the Eigen-concentration of feed spray appears at the riser center in these three different feed injection zones ( $\bar{C} \approx 0$ ), which denotes that the feed spray has not yet reached the axis of the riser because of the intense upwash by the two-phase flow coming from the prelift zone. The end of the spray appears at  $\tilde{r} = 0.32$  to  $0.54$ , because the maxima of both the Eigen-concentration and the Eigen-velocity of feed spray appear there. The deflexion angle of the spray even comes to  $20^\circ$  compared with a free jet. Near the riser wall ( $\tilde{r} = 0.86 \sim 0.95$ ), the secondary local maxima of the Eigen-concentration and the Eigen-velocity of feed spray indicate that a secondary flow of feed arises there relative to the mainstream of feed spray. The boundary between the mainstream and the secondary flow locates at  $\tilde{r} \approx 0.86$ .

At  $H = 0.675$  m above the nozzles, the maxima of both the Eigen-concentration and the Eigen-velocity of feed spray occur at  $\tilde{r} = 0$ . At the same time, the secondary local maxima of  $\bar{C}$  and  $u_c$  present at  $\tilde{r} \approx 0.75$ . It shows that the spray mainstream has already reached the riser axis and the spray secondary flow has extended gradually in this cross-section. On the other hand, the minima of the Eigen-concentration and the Eigen-velocity appear at  $\tilde{r} = 0.54$ , indicating that the boundary between the spray mainstream and the spray secondary flow has shifted to the position  $\tilde{r} = 0.54$ .

At  $H = 1.075$  m and  $H = 1.375$  m above the nozzles, the minima of the spray Eigen-concentration and the Eigen-velocity locate at the riser wall, whereas the maxima of these two parameters present at  $\tilde{r} = 0$ . It means that, at these two axial heights, the secondary flow of feed spray has disappeared. In other words, the secondary flow has merged into the mainstream.

In summary, when a feed spray is injected into the riser, a secondary flow of spray occurs. The secondary flow extends at first and then merges into the mainstream. As shown in

Figures 3 and 4, the mainstream, the secondary flow, and their boundary are illustrated by the solid line, dash line, and dash dot line, respectively.

### *The effects of feed spray on the flow pattern of particles in the feed injection zone*

We plot all the investigated flow parameters in one diagram, so that we can determine their various relationships, which are shown in Figures 5–7. It is an effective way to analyze the mixing process and the flow characteristics in the feed injection zone, although the units (or dimensions) of these parameters are different. In these figures, the unit of particle velocity is 10 m/s, while the unit of local density is  $1000 \text{ kg/m}^3$ .

If no feed spray is introduced into riser, the local density in the central region is generally lower than that in the wall region of the riser at all axial heights, presenting a typical annular-core flow as suggested by many researchers.<sup>22–30</sup> The boundary between the annular and the core located at approximately  $0.7 \leq \tilde{r} \leq 0.8$ . However, the flow pattern in the feed injection zone is different from the annular-core due to the injections of feed.

In these three different feed injection zones, the measured flow parameters present similar radial profiles, different only in magnitude, as shown in Figures 5–7. The effects of the secondary flow of feed spray on the flow pattern of particles are clearly seen in all these three investigated feed zones.

At  $H = 0.375$  m above the nozzles, based on the radial distribution of the local density, the cross-section can be divided into three radial regions: the wall dense-phase region ( $0.86 \leq \tilde{r} \leq 1$ ), the annular transition region ( $0.54 \leq \tilde{r} \leq 0.86$ ), and the central dense-phase region ( $0 \leq \tilde{r} \leq 0.54$ ). The highest density appears in the wall dense-phase region, whereas the lowest density in the annular transition region. In the annular transition region, the local density remains almost a constant in the radial direction. The occurrence of the central dense-phase region is because that numerous particles are entrained towards the central area of the riser by feed sprays. The particle backmixing is more intense in higher density areas (the wall dense-phase region and the central dense-phase region). The backmixing ratio increases with the local density. The maximum of particle velocity is at  $\tilde{r} \approx 0.32$  to  $0.54$ , corresponding to the location of spray mainstream.

As marked with the circle in Figures 5–7, the most distinct feature at  $H = 0.375$  m is that the boundary between mainstream and secondary flow coincides exactly with that of wall dense-phase region and the annular transition region, showing an evident effects of nozzle spray on the behaviors of granular flow.

At  $H = 0.675$  m above the feed nozzles, the cross-section is divided into two radial areas: the wall dense-phase region ( $0.54 \leq \tilde{r} \leq 1$ ) and the central dilute-phase region ( $0 \leq \tilde{r} \leq 0.54$ ), which resembles the annular-core to some extent. In the No. 1 feed injection zone (traditional scheme), the local density in the wall dense-phase region presents higher values and a more sharp gradient than those of a typical annular-core flow. The radial gradients of the local density in No. 2 and No. 3 zones are comparatively much flatter. At this axial height, the particle velocity distribution approaches to that of the typical annular-core flow, but the radial gradient is steeper.

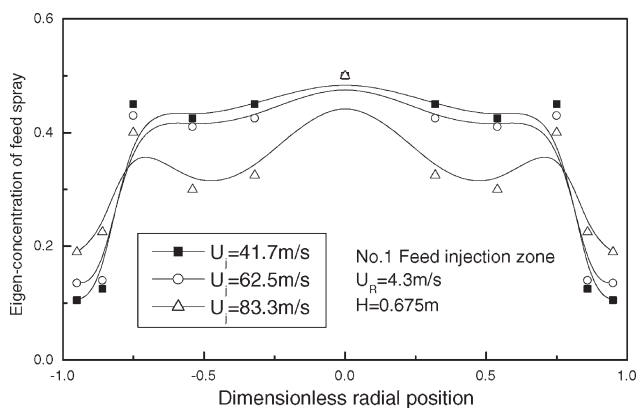


**Figure 8. Radial distributions of the Eigen-concentration of feed spray under different spray velocities.**

At  $H = 0.675$ , the maximal particle backmixing originates among these tested cross-sections, and in the wall dense-phase region in particular, the backmixing is very intense. This is because that the extension of the spray secondary flow contributes much to particles flowing transversely in this cross-section. The movement of particles resembles the flow round a blunt body, which results in the frequent collision of particles. Then, violent backmixing takes place, and a longer residence time of particles is inevitable. In the commercial riser reactors, coke often occurs at a height of 0.6 to 1 m exactly above the feed nozzles. The prevalent viewpoint about it was feed spray impinging on the opposite riser wall of the feed nozzle. However, the main cause presented in this article might be that the flow of particles performs the flow round a blunt body and the extension of the spray secondary flow.

Another salient feature at this axial height is that the boundary between the spray mainstream and the secondary flow corresponds exactly to that between the wall dense-phase region and the central dilute-phase region, as marked with the circle in Figures 5–7. The effects of feed spray, particularly, the secondary flow on the solid flow is prominent.

At  $H = 1.075$  m and  $H = 1.375$  m above the nozzles, the secondary flow of feed spray has merged into the mainstream. The cross-section is divided into two regions: the wall dense-phase region ( $0.75 \leq \tilde{r} \leq 1$ ) and the central dilute-phase region ( $0 \leq \tilde{r} \leq 0.75$ ). The particle backmixing increases or decreases depending on the variation of the local density. The maximal particle velocity locates at the riser axis, while the minimum near the wall. The radial profile of the spray Eigen-concentration coincides with the annular-core flow. In these two cross-sections, almost all inflexions of the flow parameters arise in the same position (at about  $\tilde{r} = 0.75$ ), as illustrated by the circle marked in Figures 5–7. It demonstrates that the two-phase flow approaches to the typical annular-core structure, showing that the mixing between the feed sprays and the particles has been nearly completed.

In the feed injection zone of a riser, the secondary flow of spray plays a crucial role not only in the mixing of catalysts with feed but also in the two-phase flow features. Obviously, different spray velocities will result in different extents of the secondary flow.

At the representative axial height,  $H = 0.675$  m above the feed nozzles, the radial gradient of the Eigen-concentration of feed spray decreases if increasing the spray velocity of the nozzle exit, as shown in Figure 8. This demonstrates that a higher feed spray velocity may cause a more intensive secondary flow, so that the diffusion of feed is more rapid and the mixing of feed with catalysts is enhanced consequently.

However, in a more intensive secondary flow, more particles are entrained towards the riser wall, and then, more collisions of particles take place. As a result, near the riser wall, the particle backmixing is more violent, as shown in Figure 9.

In the feed injection zone, the secondary flow of feed spray hastens the mixing of catalyst with feed oil. However, with the extension of the secondary flow, the particle backmixing is aggravated.

### *The effects of Louver conduit/baffle on the flow pattern of two-phase in the feed injection zone*

At two representative axial heights,  $H = 0.375$  m and  $H = 0.675$  m above the feed nozzles, the Eigen-concentration of feed spray in the area of  $0.54 \leq \tilde{r} \leq 1$  in the No. 2 and No. 3 feed injection zones is higher than that in the No. 1 zone, as shown in Figure 3. In other words, the radial distributions of feed spray in the No. 2 and No. 3 zones are more uniform. It also indicates that the feed spray diffuse more rapidly when a conduit or baffles is introduced.

Careful comparison of Figures 5–7 shows that in the above area, both the particle backmixing ratios and the radial gradients of the local density in the No. 2 and No. 3 zone are lower than those in the traditional zone, while the particle velocities are comparatively higher than No. 1. These are believed to be advantageous to FCC reaction. The installations of the conduit and the baffle appear desirable for improving the performance of the feed injection zone.

Based on the experimental results, it can be seen that the occurrence of the secondary flow in the No. 2 or No. 3 feed injection zone is inevitable, although the conduit or baffle is used. Furthermore, in a commercial FCC riser, the conduit or baffle has to resist the serious abrasion caused by the high-temperature multiphase flow. However, if introducing a stream of steam toward the direction of the secondary flow, i.e., setting a gaseous baffle, the secondary flow is anticipated to be effectively controlled and used. A question is

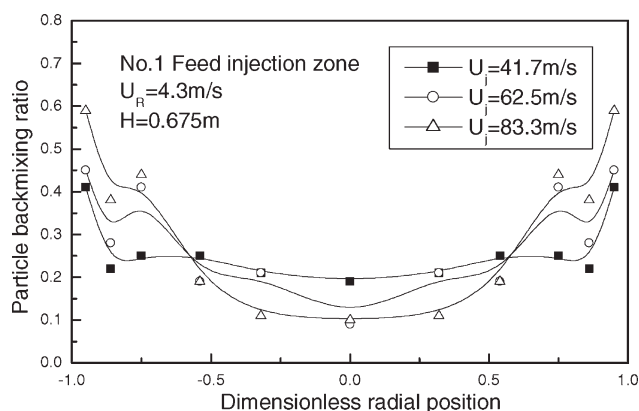


**Figure 9. Radial distributions of the particle backmixing ratio under different spray velocities.**

then put forward: where is the precise location of the secondary flow?

## Theoretical Analysis on the Generation of the Secondary Flow of Feed Spray

### The Kutta-Joukowski lift theorem

It is obvious that the occurrence of the secondary flow closely relates to a transverse force in the riser. In classical aerodynamics, a transverse force known as the Kutta-Joukowski lift has been introduced. The Kutta-Joukowski lift theorem is described as below<sup>31</sup>:

Consider a steady irrotational 2D flow past a closed body. Let the flow be uniform with a velocity  $U_\infty$  and a density  $\rho$ . Given the velocity circulation around the body is  $\Gamma$ . Then, a lift on per unit span of the body is given by as follows:

$$F_{K-J} = \rho \Gamma U_\infty \quad (1)$$

The lift is perpendicular to  $U_\infty$ , strictly speaking, turning the vector  $U_\infty$  90° reversely to the velocity circulation  $\Gamma$ .

In two-phase flow, the Saffman force and the Magnus force on particles are essentially Kutta-Joukowski lift. They are caused by the transverse gradient of the gas velocity across a particle and the rotation of the particle, respectively. However, these two forces are usually negligible, because the particles are too small.

### The Kutta-Joukowski lift in a multiphase flow

In classical single-phase hydrodynamics, the Stokes theorem has been used for any area  $A$  that is enclosed by a closed curve  $C$ . For a fluid with constant density, the velocity circulation around  $C$ ,  $\Gamma$ , is equal to the vortex strength through the area  $B$ .<sup>31</sup>

$$\Gamma = I \quad (2)$$

Consider the relation of the vortex strength  $I$  to the angular velocity  $\omega$ :<sup>31</sup>:

$$I = 2\omega_k A = 2A \times \left[ \frac{1}{2} \left( \frac{\partial U_j}{\partial X_i} - \frac{\partial U_i}{\partial X_j} \right) \right] \quad (3)$$

In single-phase hydrodynamics, the clockwise velocity circulation (or angular velocity) is negative, whereas the anti-clockwise is positive and vice versa.<sup>31</sup>

Combine Eqs. 1, 2, and 3:

$$F_{K-J} = \rho \Gamma U_\infty = \rho U_\infty A \left( \frac{\partial U_j}{\partial X_i} - \frac{\partial U_i}{\partial X_j} \right) \quad (4)$$

Then, for a multiphase flow, the Kutta-Joukowski lift exerting on Phase 2 by Phase 1 is modified by:

$$F_{K-J} = \rho_1 A (U_1 - U_2) \left( \frac{\partial U_{2j}}{\partial X_i} - \frac{\partial U_{2i}}{\partial X_j} \right) \quad (5)$$

Equation 5 establishes the relation of transverse force (Kutta-Joukowski lift) to the velocity gradient of Phase 2 in

any closed area  $A$  in a multiphase flow. In Eq. 5, the lift is a force that Phase 1 acts on Phase 2, therefore, it is closely relates to the velocity of Phase 1 relative to Phase 2  $U_1 - U_2$ . It also means that, when using Eq. 5 to analyze a multiphase flow, the term  $U_1 - U_2$  (as well as  $\frac{\partial U_{2j}}{\partial X_i} - \frac{\partial U_{2i}}{\partial X_j}$ ) is regarded as a vector, but not a scalar quantity. Then the direction of the Kutta-Joukowski lift on Phase 2 in a multiphase flow is turning the vector  $U_1 - U_2$  90° reversely to the velocity circulation.

In a confined multiphase flow, the Kutta-Joukowski lift must occur, because both the transverse velocity gradient of Phase 2 and the relative velocity of Phase 1 to Phase 2 are inevitable. Therefore, in the feed injection zone of a riser, the Kutta-Joukowski lifts exerting on feed spray by prelift gas and particles contribute much to the occurrence of the secondary flow. The direction of the lift is mainly determined by the directions of the vortex strength and the relative velocity.

### The location of the secondary flow of feed spray in riser

*The Location of the Mainstream of Feed Spray in Riser.* Although the feed injection zone of a riser is a typical 3D flow field, the analysis based on 2D can also propose some useful quantitative description for the diffusion of feed spray. Particularly, the analysis of the vortex explains the generation of the secondary flow of feed spray.

In the vicinity of the nozzle exit, a 2D orthogonal-curve coordinates is set, as illustrated by Figure 10.

In Figure 10, the Z-coordinate axis is set along the riser wall; the X-axis is vertical to Z-axis, toward the riser axis. The curve 0A represents the streamline of feed spray (mainstream), while  $\psi_0$  means the actual flow angle of feed spray in riser.  $U_z$  and  $U_x$  denote the components of the spray velocity along the Z-coordinate axis and the X-coordinate axis, respectively.

In hydrodynamics, the streamline equation is given by:<sup>31</sup>

$$\frac{dX}{h_1 dZ} = \frac{U_x}{U_z} \quad (6)$$

Here,  $h_1$  is the Lam'e coefficient of the orthogonal-curve coordinates.

In single-phase hydrodynamics, the jet in a crossflow can be modeled by a flow round a blunt body. Therefore, in the area very close to the origin of the coordinates (namely the nozzle exit),  $U_z$  and  $U_x$  is expressed by series<sup>32</sup>:

$$U_z = \left( \frac{\partial^2 U_z}{\partial X \partial Z} \right)_0 XZ + \frac{1}{2} \left( \frac{\partial^2 U_z}{\partial X^2} \right)_0 X^2 + \dots \quad (7-1)$$

$$U_x = \frac{1}{2} \left( \frac{\partial^2 U_x}{\partial X^2} \right)_0 X^2 + \dots \quad (7-2)$$

Combine Eq. 6 with Eq. 7, the equation of the streamline that passes the origin of the coordinates is as follows:

$$\frac{1}{h_1} \frac{dX}{dZ} = \frac{\left( \frac{\partial^2 U_x}{\partial X^2} \right)_0 X}{\left( \frac{2}{h_1} \frac{\partial^2 U_z}{\partial X \partial Z} \right)_0 (h_1)_0 + \left( \frac{\partial^2 U_z}{\partial X^2} \right)_0 X} \quad (8)$$

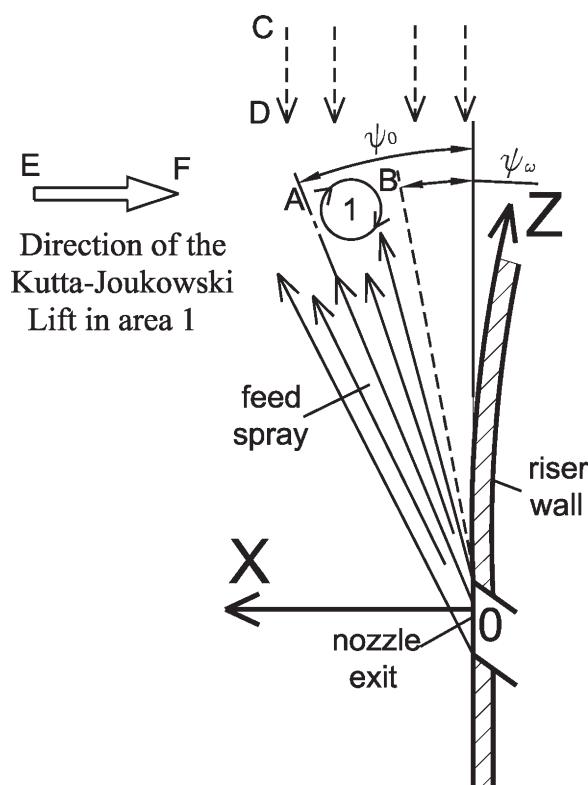


**Figure 10. A 2D orthogonal-curve coordinates in the vicinity of the nozzle exit.**

When  $(X, Z)$  is very close to the origin, we have  $\frac{1}{h_1} \frac{dX}{dZ} \approx \frac{1}{h_1} \frac{X}{Z} = \tan \psi_0$ . Transforming Eq. 8, we obtain:

$$\tan \psi_0 = \frac{\left( \frac{\partial^2 U_z}{\partial X^2} \right)_0 \tan \psi_0}{2 \left( \frac{\partial^2 U_z}{h_1 \partial X \partial Z} \right)_0 + \left( \frac{\partial^2 U_z}{\partial X^2} \right)_0 \tan \psi_0}$$

Combining above equation with the continuity equation:  $\frac{\partial U_z}{h_1 \partial Z} + \frac{\partial U_x}{\partial X} = 0$ , we have:

$$\tan \psi_0 = \frac{\left( \frac{\partial^2 U_x}{\partial X^2} \right)_0 - 2 \left( \frac{\partial^2 U_z}{h_1 \partial X \partial Z} \right)_0}{\left( \frac{\partial^2 U_z}{\partial X^2} \right)_0} = - \frac{3 \left( \frac{\partial^2 U_z}{h_1 \partial X \partial Z} \right)_0}{\left( \frac{\partial^2 U_z}{\partial X^2} \right)_0} \quad (9)$$

Thus, in the area very close to the nozzle exit, the relation of the actual flow angle of feed spray in riser to the velocity gradients is given by Eq. 9. It also represents the streamline equation of feed spray (mainstream).

**The Zero-Vortex-Strength Curve.** The vortex strength is  $I = 2\omega A = \frac{1}{2} \left[ \left( \frac{\partial U_x}{h_1 \partial Z} \right) - \frac{\partial U_z}{\partial X} \right] 2A$ . Here  $A$  means any closed area. Consider a curve along which the vortex strength is equal to zero. Based on Eqs. 2, 3, and 4, the Kutta-Joukowski lift along the zero-vortex-strength curve is zero too. It means that in the vicinity of the nozzle exit, there must be a flow along this curve without interference of the transverse force. As described in the following text, it closely relates to the location of the secondary flow of feed spray.

Combine the definition of the vortex strength with Eq. 7, i.e., along the zero-vortex-strength curve, we get the following:

$$\omega = - \left[ \left( \frac{\partial^2 U_z}{\partial X \partial Z} \right)_0 Z + \left( \frac{\partial^2 U_z}{\partial X^2} \right)_0 X + \dots \right] = 0$$

In the area very close to the origin of the coordinates, the tangent of the zero-vortex-strength curve is as follows:

$$\tan \psi_\omega = - \frac{\left( \frac{\partial^2 U_z}{h_1 \partial X \partial Z} \right)_0}{\left( \frac{\partial^2 U_z}{\partial X^2} \right)_0} = \frac{1}{3} \tan \psi_0 \quad (10)$$

The location of the zero-vortex-strength curve is illustrated by OB in Figure 10.

**The Location of the Secondary Flow of Feed Spray in Riser.** Experimental results show that the secondary flow of feed spray locates between the riser wall and the spray mainstream. The generation of the secondary flow requires a transverse force whose direction is toward the riser wall, as shown by the arrow EF in Figure 10.

The spray velocity at the nozzle exit is much higher than those of the prelift gas and the particle flow in FCC riser. In the vicinity of the nozzle exit, the component  $U_z$  is also higher than the prelift gas velocity  $U_R$  and the particle velocity  $V_p$ . In other words, as shown in Figure 10, the direction of  $U_R$  (or  $V_p$ ) relative to  $U_z$  is negative value (down direction). Namely, the direction of  $U_R - U_z$  or of  $V_p - U_z$  is illustrated by the arrow CD.

Thus, according to the Kutta-Joukowski lift theorem, generating a transverse force toward the riser wall requires negative vortex strength (or a clockwise velocity circulation as illustrated by the circle 1 in Figure 10). In the area between OA and OB, the velocity of the spray inevitably decreases along the riser height because of the underwashing by the two-phase flow coming from the prelift zone. Hence,  $\frac{1}{2} \left( \frac{\partial U_x}{h_1 \partial Z} \right)$  is negative. On the other hand,  $\frac{\partial U_z}{\partial X}$  is positive, because the direction of X-coordinate axis is toward the center of the spray, and the velocity at the central line of a jet is undoubtedly higher than that near the jet boundary. Hence,  $\omega = \frac{1}{2} \left( \frac{\partial U_x}{h_1 \partial Z} \right) - \frac{\partial U_z}{\partial X}$  is negative. Therefore, in the area between OA and OB, the direction of the Kutta-Joukowski lift on feed spray is toward the riser wall. It is the Kutta-Joukowski lift that causes the generation and extension of the secondary flow of feed spray.

Based on experimental results, we can see that the angle  $\psi_\omega$  is exactly corresponding to the location of the spray secondary flow. In other words, the relation of the orientation of the secondary flow to that of the mainstream satisfies  $\tan \psi_\omega = \frac{1}{3} \tan \psi_0$  (see Appendix).

The Kutta-Joukowski lift theorem can also be used to explain the generation of the annular-core flow in a riser. In Figure 11, the lift of gas/liquid phase exerting on solid phase is analyzed. The velocity of the lift gas/liquid relative to the particles is positive value (up direction), as illustrated by the arrow CD (here the relative velocity is considered as a vector. Even in the vicinity of the riser wall, the relative velocity is still positive value because of the no slip condition for the gas/liquid and the downflow of particles.). In the fully developed zone of a riser, the gradients of particle velocity conform to  $\frac{\partial V_{pz}}{\partial Z} = 0$  and  $\frac{\partial V_{pz}}{\partial r} < 0$ , then  $\omega_\theta = \frac{1}{2} \left( \frac{\partial V_{pz}}{\partial Z} \right) - \frac{\partial V_{pz}}{\partial r} > 0$ . The vortex strength  $\omega_\theta$  is positive, corresponding to an anticlockwise velocity circulation as illustrated by the circle 1 in Figure 11. Therefore, the direction of the Kutta-Joukowski lift on particles is towards the riser wall.



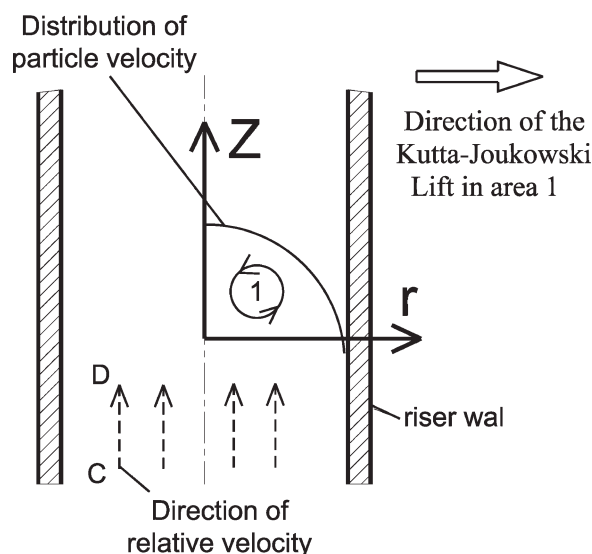


**Figure 11. Schematic diagram of using Kutta-Joukowski lift theorem to analyze the radial profile of local density in a riser.**

Here, the zero-vortex-strength curve locates at the riser axis, because both  $\frac{\partial v_{\theta r}}{\partial z}$  and  $\frac{\partial v_{\theta z}}{\partial r}$  are equal to zero at the riser center. There is no transverse force acting upon the particles.

The quantitative effect of the Kutta-Joukowski lift on the radial profile of the local density will be presented in detail in a future article.

### Improving the Contact of Feed Oil with Catalysts in FCC Riser

As preceding description, the importance of the secondary flow is obvious. It greatly improves the mixing of catalysts and feed spray. On the other hand, the location of the feed secondary flow corresponds to the particle dense-phase region in which the particle axial velocity is relatively low, and if the backmixing is violent, it is believed to be harmful to FCC reaction. Therefore, effectively controlling and utilizing the secondary flow is the key factor to improve the contact of feed oil with catalysts in FCC riser.

The schematic diagram of a novel feed nozzle is given in Figure 12. Two adjacent exits are set at the head of the nozzle. One is the usual exit of feed spray; the other is an exit of a stream of auxiliary steam.

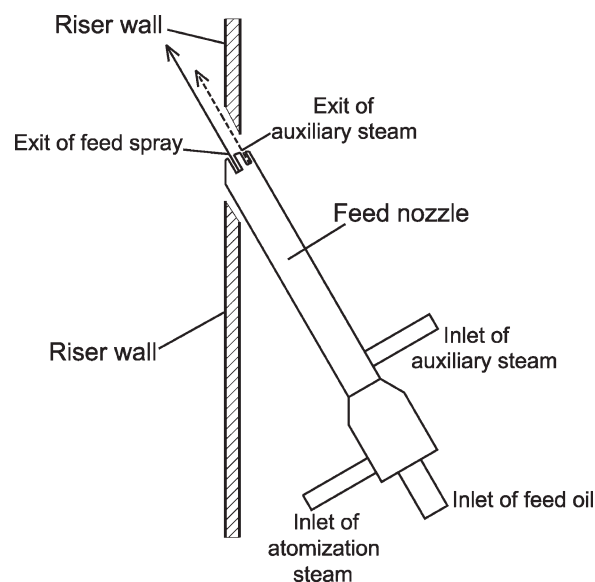


**Figure 12. A schematic diagram of the feed nozzle which can control and use the secondary flow in riser.**

steam is allocated as the auxiliary steam which is used to control the secondary flow of feed spray in FCC riser, corresponding to the *gaseous* baffle mentioned above. The injection angle of the auxiliary steam is determined by Eq. 10, exactly toward that of the secondary flow.<sup>33-34</sup>

In a commercial FCC unit, when feed oil is injected into the riser, the oil droplets are instantaneously vaporized. In other words, the feed are transformed from liquid phase to gas phase promptly. Because the relaxation time of gas-gas is much shorter than that of gas-solid, so the auxiliary steam is easily syncrized or entrained with the feed gas. At the same time, a part of catalysts that were carried by the secondary flow is blown off the riser wall by the auxiliary steam. As a result, the backmixing of catalysts are effectively controlled while the diffusion rate of feed spray is not weakened. Thus, the secondary flow are controlled and used.

As illustrated in Table 1, the effects of the proposed nozzle used in some commercial FCC units are quite desirable. The liquid yield, i.e., the total yields of gasoline, LPG and diesel increases considerably, while some undesirable byproducts such as the dry gas and coke decrease.

**Table 1. Effects of the Nozzle with Auxiliary Steam Used in Several Commercial FCC Units**

	Capacity (Mt/a)	Liquid Yield (Gasoline + LPG + Diesel, %)	Dry Gas (%)	Coke (%)
Fushun Petro Co. (1), China	1.20	+2.07	-0.83	-0.88
Fushun Petro Co. (2), China	2.07	+1.54	-0.83	-1.24
Nanchong Petro Co., China	0.40	+1.48	-0.68	-0.20
Jilin Petro Co. (1), China	0.70	+0.91		
Jilin Petro Co. (2), China	1.00	+2.25	0	-0.05
Jinan Petro Co., China	1.40		-0.77	
Changling Petro Co., China	1.20			-1
Gaoqiao Petro Co., China	0.60	+1.37		
Jinzhou Petro Co., China	0.80	+0.68		
Jinling Petro Co., China	1.30	+2.84		
Jinxi Petro Co., China	1.00	+1.20		
Qingdao Petro Co., China	1.40	+1.29		

## Conclusion

In a large cold-riser model, the diffusion pattern of feed spray, as well as the flow features of catalysts, in three different-structure feed injection zones is experimentally investigated.

When feed oil injected into the riser, the flow features of the gas–solid two-phase are much different from the typical annular-core structure. A secondary flow of feed spray occurs. The secondary flow extends at first and then merges into the mainstream. The secondary flow improves the mixing of catalysts and feed. However, the extension of the secondary flow causes violent catalysts backmixing; it is believed to be harmful to FCC reaction.

The generation of the secondary flow is theoretically analyzed by using Kutta-Joukowski lift theorem. The location of the secondary flow is quantified; it corresponds to a zero-vortex-strength curve:  $\tan \psi_\omega = \frac{1}{3} \tan \psi_0$ .

A novel FCC feed nozzle, which can control/utilize the secondary flow of feed spray in riser, is introduced. The effects of this type of nozzle used in some commercial FCC units are evident.

## Acknowledgments

The authors gratefully acknowledge the supports from the National Natural Science Fund of China: National Science Fund for Distinguished Scholars No. 20525621, No. 20725620, Key Program No. 20490200 and General Programs No. 20576076, No. 20676147.

## Notation

$A$  = area,  $m^2$   
 $C_i$  = tracer concentration at  $i$  position  
 $\bar{C}$  = Eigen-concentration of feed spray  
 $D$  = diameter of riser,  $m$   
 $d_p$  = mean diameter of particles,  $\mu m$   
 $dA$  = any differential area,  $m^2$   
 $F_{K-J}$  = Kutta-Joukowski lift,  $N/m$   
 $G_s$  = mass flux of particles in riser,  $kg/m^2s$   
 $H$  = height above the nozzles,  $m$   
 $I$  = vortex strength,  $m^2/s$   
 $k$  = constant  
 $n_d$  = number of the particles whose velocity is downward  
 $n_u$  = number of the particles whose velocity is upward  
 $Q_j$  = total gas flowrate of four nozzle sprays,  $m^3/s$   
 $Q_R$  = gas flowrate of prelift gas,  $m^3/s$   
 $R$  = radius of riser,  $m$   
 $r$  = radial position,  $m$   
 $t$  = mean residence time of the hydrogen tracer at the sampling position,  $s$   
 $u_c$  = Eigen-velocity of feed spray in riser,  $m/s$   
 $U$  = velocity of gas,  $m/s$   
 $U_R$  = superficial velocity of the prelift gas,  $m/s$   
 $U_j$  = spray velocity at the nozzle exit,  $m/s$   
 $U_x$  = components of the spray velocity along the  $X$ -coordinate in riser,  $m/s$   
 $U_z$  = components of the spray velocity along the  $Z$ -coordinate in riser,  $m/s$   
 $U_\infty$  = velocity of a steady irrotational 2D single-phase flow in the Kutta-Joukowski Lift Theorem,  $m/s$   
 $V_p$  = velocity of particle,  $m/s$   
 $V_{p,r}$  = velocity of particle along the  $r$  direction,  $m/s$   
 $V_{p,z}$  = velocity of particle along the  $z$  direction,  $m/s$   
 $V_d$  = mean velocity of the particles whose velocity is downward,  $m/s$   
 $V_u$  = mean velocity of the particles whose velocity is upward,  $m/s$   
 $X$  = the coordinate vertical to  $Z$  coordinate, towards the riser axis,  $m$   
 $X_i$  =  $i$ th coordinate direction,  $m$   
 $X_j$  =  $j$ th coordinate direction,  $m$   
 $Z$  = axial height of the riser,  $m$

## Greek letters

$\alpha$  = attack angle of the Louver conduit in the No. 2 feed injection zone, or of the baffle in the No. 3 feed injection zone  
 $\beta$  = divergence angle of the Louver conduit in the No. 2 feed injection zone, or of the baffle in the No. 3 feed injection zone  
 $\varepsilon_{pi}$  = local volume fraction of particles measured at  $i$  position  
 $\rho$  = density of a steady irrotational 2D single-phase flow in the Kutta-Joukowski Lift Theorem,  $kg/m^3$   
 $\rho_p$  = density of particle,  $kg/m^3$   
 $\psi_0$  = actual flow angle of the mainstream of feed spray in riser  
 $\psi_\omega$  = flow angle of the secondary flow of feed spray in riser; the angle of the zero-vortex-strength curve  
 $\gamma$  = particle backmixing ratio  
 $\Gamma$  = velocity circulation,  $m^2/s$   
 $\omega$  = angular velocity,  $1/s$

## Subscript

0 = the mainstream of feed spray in riser  
 $i$  =  $i$ th coordinate; position  $i$   
 $j$  =  $j$ th coordinate; nozzle spray gas  
 $k$  =  $k$ th coordinate  
 $p$  = particle  
 $R$  = prelift gas  
 $r$  = radial  
 $Z$  = axial  
 $\omega$  = the secondary flow of feed spray in riser; vortices strength is equal to zero

## Literature Cited

- Chen YM. Recent advances in FCC technology. *Powder Technol.* 2006;163:2–8.
- Helmsing MP, Makkee M, Moulijn JA. Short contact time experiments in a novel benchscale FCC riser reactor. *Chem Eng Sci.* 1996;51:3039–3044.
- Dupain X, Makkee M, Moulijn JA. Optimal conditions in fluid catalytic cracking: a mechanistic approach. *Appl Catal.* 2006;297:198–219.
- McMilan J, Zhou D, Saberian M, Briens C, Berruti F. Measurement techniques to characterize the contact between injected liquid and circulating solids in downer mixing chamber. *Powder Technol.* 2006;161:175–184.
- Fan Y, Ye S, Chao Z, Lu C, Sun G, Shi M. Gas-solid two-phase flow in FCC riser. *AIChE J.* 2002;48:1869–1887.
- Thelogs KN, Lygeros AI, Markatos NC. Feedstock atomization effects on FCC riser reactor selectivity. *Chem Eng Sci.* 1999;54:5617–5625.
- Thelogs KN, Markatos NC. Advanced modeling of fluid catalytic cracking riser-type reactors. *AIChE J.* 1993;39:1007–1014.
- Thelogs KN, Nikou I, Lygeros AI, Markatos NC. Simulation and design of fluid catalytic cracking riser-type reactors. *AIChE J.* 1997;43:486–498.
- Thelogs KN, Nikou I, Lygeros AI, Markatos NC. Simulation and design of fluid-catalytic cracking riser-type reactors. *Comput Chem Eng.* 1996;20:S757–S762.
- Gao J. *Numerical Simulation on the Flow, Heat-Transfer and Reaction in the Catalytic Cracking Riser Reactors*. Ph.D. Thesis. Beijing, China University of Petroleum, 1997.
- Albrecht A, Simonin O, Barthod D, Vedrine D. Multidimensional numerical simulation of the liquid feed injection in a industrial FCC riser. *CFB-10 preprints*. 2001:349–359.
- Maroy JD. *Process and Apparatus For Contacting a Hydrocarbon Feedstock with the Hot Solid Particles in Tubular Reactor with a Rising Fluidized Bed*. U.S. Patent 5,348,644, 1994.
- Zheng M, Hou S, Zhong X, Li S. Determining the particle velocity distribution in FCC riser with different structures. *Pet Process Petrochem (in China)*. 2000;31:45–51.
- Dries HWA. *Reactor Riser for Fluidized-Bed Catalytic Cracking Plant*. U.S. Patent 6,596,242, 2003.
- Lomas DA. *FCC Riser with Transverse Feed Injection*. U.S. Patent 5,139,748, 1992.
- Maulon JL, Demar M, Sigaud JB. *The Method for the Injection of Catalyst in a Fluid Catalytic Cracking Process, Especially for Heavy Feedstock*. U.S. Patent 4,832,825, 1989.

17. Chen YM. *Feed Nozzle*. U.S. Patent 5,794,857, 1998.
18. Chen YM. *Feed Nozzle*. U.S. Patent 5,979,799, 1999.
19. Zhang H, Johnston P, Zhu J, Lasa H, Bergougnou M. A novel calibration for an optical fiber solid concentration probe. *Powder Technol.* 1998;100:260–272.
20. Zhu J, Li G, Qin S, Li F, Zhang H, Yang Y. Direct measurement of particle velocities in gas-solid suspension flowing using a novel five-optical fiber probe. *Powder Technol.* 2001;115:184–192.
21. Werther J, Hage B, Rudnick C. A comparison of laser Doppler and single-fiber reflection probes for the measurement of the velocity of solid in a gas-solid fluidized bed. *Chem Eng Process.* 1996;35:381–391.
22. Miller A, Gidaspow D. Dense, vertical gas-solid flow in a pipe. *AIChE J.* 1992;38:1801–1815.
23. Aguillon J, Shakourzadeh K, Guigon P. A new method for local solid concentration measurement in circulating fluidized bed. *Powder Technol.* 1996;86:251–255.
24. Zhang W, Tung Y, Johnsson F. Radial voidage profiles in fast fluidized beds of different diameters. *Chem Eng Sci.* 1991;46:3045–3052.
25. Nieuwland J, Meijer R, Kuipers J, van Swaaij W. Measurement of solid concentration and axial solid velocity in gas-solid two-phase flows. *Powder Technol.* 1996;87:127–139.
26. Wei F, Lin H, Cheng Y, Wang Z, Jin Y. Profiles of particle velocity and solid fraction in a high-density riser. *Powder Technol.* 1998;100:183–189.
27. Issangya A, Bai D, Bi H, Lim K, Zhu J, Grace J. Suspension densities in a high-density circulating fluidized bed riser. *Chem Eng Sci.* 1999;54:5451–5460.
28. Issangya A, Grace J, Bai D, Zhu J. Further measurement of flow dynamics in a high-density circulating fluidized bed riser. *Powder Technol.* 2000;111:104–113.
29. Zhang H, Huang W, Zhu J. Gas-solid flow behavior: CFB riser vs. Downer. *AIChE J.* 2001;47:2000–2011.
30. Pärssinen J, Zhu J. Axial and radial solid distribution in a long and high-flux CFB riser. *AIChE J.* 2001;47:2197–2205.
31. Jiang H. *Hydromechanics*. Xi'an, China: Xi'an Jiaotong University Press, 1985:89–97.
32. Zhang H. *The Topological Structure Analysis on the Separation Flow & Vortices Movement*. Beijing: National Defense Industry Press, 2002:3–7.
33. Chen Q, Fan Y, Wu C, Chen W, Xu D. *FCC Feed Nozzle*. China Patent ZL200410010045.3, 2006.
34. Chen Q, Fan Y, Wu C, Chen W, Xu D. *FCC Feed Nozzle*. China Patent ZL200420010123.5, 2005.

## Appendix: Verification on the Relation of the Orientation of the Secondary Flow to that of the Mainstream

### The location of the secondary flow of feed spray in the No. 1 feed injection zone

At  $H = 0.375$  m above the nozzles, the mainstream of feed spray appears at the position  $\tilde{r} \approx 0.54$ , so the tangent of the actual flow angle of the spray mainstream is as follows:

$$\begin{aligned} \operatorname{tg} \psi_0 &= \frac{(D/2) \times (1 - \tilde{r}_{\text{spray mainstream}})}{H=0.375} \\ &= \frac{0.093 \times (1 - 0.54)}{0.375} = 0.114 \end{aligned}$$

The tangent of the flow angle of the spray secondary flow is determined according to the position of the secondary flow at  $H = 0.675$  m above the nozzles, because the precise location of the secondary flow at this height seems much more legible than that at the height of 0.375 m.

At  $H = 0.675$  m, the spray secondary flow appears approximately at the position of  $\tilde{r} \approx 0.75$ . Then:

$$\begin{aligned} \operatorname{tg} \psi_\omega &= \frac{(D/2) \times (1 - \tilde{r}_{\text{spray secondary flow}})}{H=0.675} = \frac{0.093 \times (1 - 0.75)}{0.675} \\ &= 0.035; \operatorname{tg} \psi_\omega \approx \frac{1}{3} \operatorname{tg} \psi_0 \end{aligned}$$

### The location of the secondary flow of feed spray in the No. 2 and No3 feed injection zones

In the No. 2 or No. 3 feed injection zone, the attack angle of the Louver conduit or of the baffle is  $2.5^\circ$  relative to the riser axis.

In both of these two feed injection zones, at  $H = 0.375$  m above the nozzles, the mainstream of feed spray appears at the position  $\tilde{r} \approx 0.54$ . Therefore, the tangent of the actual flow angle of the feed spray mainstream is as follows:

$$\begin{aligned} \operatorname{tg} \psi_0 &= \frac{(D/2 - 0.375 \times \operatorname{tg} 2.5^\circ) \times (1 - \tilde{r}_{\text{spray mainstream}})}{H=0.375} \\ &= \frac{(0.093 - 0.375 \times \operatorname{tg} 2.5^\circ) \times (1 - 0.54)}{0.375} = 0.094 \end{aligned}$$

In both of these two feed injection zones, the axial height of 0.675 m locates above the Louver conduit (or above the baffle). Both the mainstream and the secondary flow of feed inevitably veer when they pass through the Louver conduit (or through the baffle). So the tangent of the flow angle of the spray secondary flow is determined according to the location of the secondary flow at  $H = 0.375$  m.

In both of these two feed injection zones, at  $H = 0.375$  m, the spray secondary flow appears approximately at the position of  $\tilde{r} \approx 0.86$ . Then:

$$\begin{aligned} \operatorname{tg} \psi_\omega &= \frac{(D/2 - 0.375 \times \operatorname{tg} 2.5^\circ) \times (1 - \tilde{r}_{\text{spray secondary flow}})}{H=0.375} \\ &= \frac{(0.093 - 0.375 \times \operatorname{tg} 2.5^\circ) \times (1 - 0.86)}{0.375} = 0.029 \\ \operatorname{tg} \psi_\omega &\approx \frac{1}{3} \operatorname{tg} \psi_0 \end{aligned}$$

Manuscript received Nov. 4, 2008, and revision received June 2, 2009.